71st International Astronautical Congress (IAC) – The CyberSpace Edition, 12-14 October 2020.

IAC–20,A6,7,7,x58709

Automated Operations for the Maintenance of a Space Object Database

Benedikt Reihs[1,*], Alessandro Vananti[1], Thomas Schildknecht[1], Jan Siminski[2], and Tim Flohrer[3]

[1]Astronomical Institute University of Bern (AIUB), Sidlerstrasse 5, 3012 Bern, Switzerland
[2]IMS Space Consultancy, ESA/ESOC, Robert-Bosch-Str 5, 64293 Darmstadt, Germany
[3]ESA/ESOC, Robert-Bosch-Str 5, 64293 Darmstadt, Germany
[*]Corresponding Author: benedikt.reihs@aiub.unibe.ch

Abstract

To cope with the increasing number of objects in space around Earth, the processing of observations of these objects shall be automated as much as possible. In this work, the automation of three parts of the maintenance of a space object orbit database, commonly called catalogue, is analysed. The first one is the association of new measurements with stored orbits in the database based on a comparison in a common coordinate frame using the Mahalanobis distance under the assumption of normally distributed errors. It is shown for radar observations, that making this comparison in either the observation or orbit coordinates is only feasible if the error in the transformed system is small enough to remain normal after the transformation. Additional work is dedicated to derive a quality measure from the orbit state and covariance to give feedback, which also considers new measurements, on the current status or quality of an object in the database. Different concepts from information theory, namely the entropy and the surprisal, are tested and found to be useful quantities for these tasks. Future work will need to extend these parameters to consider further information and test their robustness with large data sets.

Keywords: database maintenance, correlation, automation

1 Introduction

The continuous increase of the number of objects in space including both active payloads and debris is a challenge for the safe operation of satellites [1]. One of the keys to space safety with regard to the space object population is the maintenance of a database containing their orbital information, commonly called catalogue. This database can be used for various tasks, e.g. collision avoidance or re-entry predictions. In order to maintain such a database, it is necessary to regularly process new observations. This includes the association of new observations to orbits in the database as well as creating new entries for previously uncatalogued objects, for example by attempting to associate observations among each other using those observations which could not be associated to a database object in the first step. With regard to the possibly large number of objects in such a database, these tasks should be performed with as much autonomy as possible.

In the following, it is assumed that a sensor provides so-called tracklets to the catalogue. A tracklet is a sequence of observations from a single object during a pass measured from a single station. In this paper, mainly radar sensors are considered as a source of the data. The observables of the radar are defined as the range ρ, the range-rate $\dot{\rho}$, azimuth az and elevation el.

The following analysis considers different steps for the build-up of a database. The association of a tracklet to a catalogue orbit will be analysed first, because it is a prerequisite for the maintenance of a

catalogue. Afterwards, the confirmation of objects is based on the assumption that a pairwise association of uncorrelated tracklets has been performed, see e.g. [2], and for simplicity it is also assumed that these initial correlations are correct. An object shall be confirmed if it has a sufficient quality after the orbit determination from the initial correlations and this quality measure shall also be used to monitor existing catalogue objects. Here, the term *quality* refers to having an orbit which fulfils a performance criterion depending on the application of the catalogue, e.g. it is accurate enough to allow a confident association of subsequent measurements over a defined period of time.

2 Tracklet-Catalogue Association

2.1 Problem Statement

For this part of the paper, it is assumed that a database of space objects already exists, which contains orbits and their covariances. If new measurements are received, it shall be tested whether they originate from an object in the catalogue by comparing the stored orbits to the measurements. The uncertainties of the measurements are also assumed to be known. The association between a catalogue orbit and a tracklet is performed by transforming the measurement and the orbit, propagated to the measurement epoch, including their uncertainties into the same coordinate system for a comparison. The importance of the selection of this coordinate system is due to the transformation of the covariance matrices, which are assumed to be Gaussian in the original system and shall maintain their normality after the transformation. For example, the transformation between the measurement system and the orbit state is usually non-linear and thus for large uncertainties of the orbit this transformation may not lead to a good representation of the covariance in measurement space. Practically, this also depends on the observation geometry and the dynamics of the observed objects.

If both distributions are in the same coordinate system, which may require the transformation of at least one of them, one possible measure to compare them is the Mahalanobis distance. It is based on a multivariate normal distribution $\mathcal{N}(\vec{x}|\vec{\mu},\Sigma)$ with mean $\vec{\mu}$ and covariance matrix Σ and it is defined as the distance from the mean $\Delta\vec{x} = \vec{x} - \vec{\mu}$ normalised by its covariance matrix [3]:

$$M_\mathrm{d} = \sqrt{\Delta\vec{x}^T \cdot \Sigma^{-1} \cdot \Delta\vec{x}}\ . \tag{1}$$

If two different normal distributions $\mathcal{N}_1$ and $\mathcal{N}_2$ shall be tested whether they could have the same mean value, the used values are $\Delta\vec{x} = \vec{\mu}_1 - \vec{\mu}_2$ and $\Sigma = \Sigma_1 + \Sigma_2$. The Mahalanobis distance is χ-distributed and thus allows statistical gating. Thus, if the Mahalanobis distance is below a given threshold, the two distributions are assumed to have the same mean, which in this case means the correlation of the two distributions is accepted.

Because the orbit's state vector can be transformed into the standard radar and optical observables, making the association in the measurement space is always possible. The use of other systems for the comparison depends on the observables and is discussed in the following separately for optical and radar observations. In case of optical measurements, it is not possible to directly transform the observables into the position-velocity state space of the orbit, because the range to the detected object is missing to derive its position. In order to compensate this, one can assume that the range is equivalent to the expected value at the measurement epoch based on the catalogue orbit. Alternatively, the optical measurements can be projected onto the orbital plane and the corresponding position is used to estimate the range [4]. The difference to the catalogue state is calculated in the cartesian RTN coordinate system, which originates in the object's current cartesian position. Its first axis is aligned with the radius vector and the second axis points orthogonally in the direction of motion, but depending on the orbit's eccentricity it may not be aligned exactly with the velocity vector. This approach was extended by [5] using a curvilinear coordinate system according to [6]. In this case, the projection of the optical measurement into a full state is found by either searching for a state which sets the radial position and velocity differences from the catalogue orbit to zero or by directly minimising the Mahalanobis distance between measured and expected position. These approaches are useful if the orbit uncertainties are large and the observation geometry is such that the transformation from the orbit state to the measurement space is highly non-linear which affects the mapping of the covariance onto the measurement space.

Considering radar observations, the range is part of the measurement and thus an inertial cartesian position can be derived directly from the measurements. The catalogue state and the measured position can be compared directly in a cartesian or curvilinear RTN coordinate system. Another option is to derive an initial orbit from the new tracklet and, instead of using the position-velocity space, compare the two orbits in their element-space, see e.g. [7, 8]. However, if there is only a single or very few

detections during the pass, there is no good chance of obtaining a reliable orbit.

Apart from using the Mahalanobis distance, [7] describes a fixed gating approach for radar measurements based on the differences between the measured and predicted positions in RTN coordinates without considering the covariances. Another approach is to calculate the divergence between two probability distributions, here measurement and state, to decide whether they belong to the same object, see e.g. [9, 10].

2.2 Association Test

The following analysis focuses on radar measurements and the association decision is taken via the Mahalanobis distance in a common coordinate frame, which can be derived directly from the detection without an orbit determination. The resulting problem is to find an appropriate frame for this comparison. The difficulty of finding a good frame for the comparison is due to the overlapping effects of the measurement and orbit errors.

As an example, consider an object in an orbit with a semi-major axis $a = 6\ 878$ km, an eccentricity $e = 0.001$, and an inclination $i = 86°$ which is detected at a range $\rho = 544$ km and an elevation $el = 67°$. The position uncertainty in the orbit's curvilinear RTN frame is $[0.01, 15.0, 0.01]$ km and the measurement uncertainties are [$\sigma_\rho = 0.01$ km, $\sigma_{\dot{\rho}} = 0.01$ km/s, $\sigma_{az,el} = 1.0°$]. The assumed uncertainties are mainly dominated by the along-track error of the orbit and the angular error of the radar. Figure 1a shows the resulting distribution of measurements from a Monte Carlo experiment using the mentioned uncertainties projected into the cartesian TR-plane and it appears to be well-shaped as no distortions are visible in this plot. To explain how this cloud of points is created, Figure 1b separates the effects of the orbit and the sensor noise and shows a cut through the TR-plane at N=0 km. For the orbit noise, it is visible that the large along-track error makes the curvature of the orbit visible leading to a non-normal distribution in this frame. The second set of points shows the effect of the radar noise. This distribution is tilted and curved, thus also not normal in the given frame. The distribution of the radar noise is highly dependent on the observation geometry but this plot allows it to deduce that there is no frame which can fit both distributions to be normal.

For the following tests, a catalogue state is assumed to be known including the orbit and its covariance. Based on this state as a reference, the true and to the observer unknown position of the object is obtained by corrupting the catalogue state with different levels of orbit noise in the curvilinear RTN frame according to its covariance. Thus, it is implicitly assumed that the covariance in the catalogue is realistic. Measurements with the given sensor noise are derived from the true state. The squared Mahalanobis distance M_d^2 is calculated between the measurement and the catalogue state in different coordinate systems. If this is performed for a large set of observations, the resulting distribution of M_d^2 should follow a $\chi^2(\nu)$-distribution with the degrees of freedom ν equal to the number of compared variables per observations. The degrees of freedom are $\nu = 4$ for the direct use of the radar observations $(\rho, \dot{\rho}, az, el)$ and $\nu = 3$ for the comparison of RTN positions. Different statistical parameters are derived from the M_d^2-distribution and compared to the theoretical values of the $\chi^2(\nu)$-distribution. Those parameters are the mean ($\mu = \nu$), the median $m \approx \nu \cdot \left(1 - \frac{2}{9\nu}\right)^3$ and the variance ($\sigma^2 = 2\nu$) [11]. Additionally, the threshold values of $\chi^2(\nu)$ are checked for which there should be a cumulative value of 5% and 95% of the samples to test both ends of the distribution for a possible shift of the values. The threshold at 99.9% of the $\chi^2(\nu)$-distribution is checked to detect the frequency of outliers. These outliers are removed for the calculation of the remaining statistical properties to increase the robustness of these parameters. Thus, this outlier rate should be at 0.1% which represents the most strict condition as can be seen in the following. The resulting heatmaps depict the difference between the value obtained from the sampled distribution and the theoretically expected one.

This experiment uses a population of 1 000 different objects in Low Earth Orbit (LEO) for a simulation of observations from a single station over seven days. This leads to approximately 25 000 passes in total. To limit the computational time, 2 500 passes are randomly selected for the following tests. Each test uses the same set of passes. The noise values are set to $[0.01, \sigma_\mathrm{T}, 0.01]$ km in the orbit's curvilinear RTN frame and [$\sigma_\rho = 0.02$ km, $\sigma_{\dot{\rho}} = 0.01$ km/s, $\sigma_{az,el}$] for the measurements. The dominating noise values σ_T and $\sigma_{az,el}$ are varied systematically. Only true positive correlations are tested to analyse the resulting distribution.

The following tests can be separated further into two sub-categories: single-point association and multi-point association. Single-point association refers to those methods which can be performed with a single detection, here the association in measurement space and curvilinear RTN, see Section 2.2.1 and Section 2.2.2. In contrast to that, the

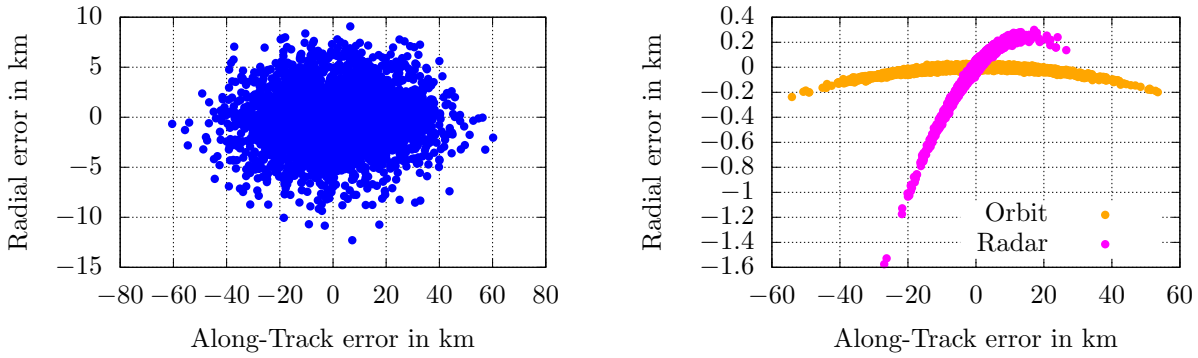

(a) Combined

(b) Single sources

Figure 1: Distribution of measured positions by combining the noise of the radar and the orbit's position uncertainty. (b) is cut along RT-plane

multi-point association requires a sequence of detections, here the time bias removal, see Section 2.2.3 and Section 2.2.4. Those also add another dimension to the problem because the results may also be dependent on the number and spacing of the observations.

2.2.1 Observations

The first experiment uses the observables directly. The association is performed by comparing the measured observables $(\rho, \dot{\rho}, az, el)$ to those expected from the catalogue state. Combining their difference with the sum of the measurement covariance and the orbit covariance transformed into the measurement system, the Mahalanobis distances can be calculated. The distribution of the resulting distances of the entire population is compared to the expected values of the $\chi^2(4)$-distribution and the differences between them are shown in Figure 2. Figure 2a contains the percentage of outliers. This number becomes significantly larger than 0.1% for along-track errors of more than 5 km. For the remaining parameters, it might be argued that the association is acceptable for up to 7.5 km along-track (AT) uncertainty. All parameters show roughly constant results for the same AT value, whereas the differences continuously increase for increasing AT uncertainties at a constant sensor noise. This behaviour confirms that this coordinate system is not sufficient for large AT uncertainties due to the nonlinearity of the transformation into the measurement system, which increases its effect with an increasing size of the orbit covariance. It should also be considered, that for a sensor with a very low sensor noise ($\sigma_{az,el} = 0.001°$), the sensitivity to the along-track noise is much higher with the degradation starting already at $\sigma_{\mathrm{T}} \approx 1$ km, because the orbit error is dominating compared to the very small measurement error.

2.2.2 Curvilinear RTN

The observations (ρ, az, el) and their covariance matrix are transformed into the orbit's curvilinear RTN system to perform the association in this system. This system can, as one would expect, tolerate also large along-track uncertainties. In contrast to the cartesian RTN, it considers the curvature of the orbit for a growing along track error [6]. As visible in Figure 3, the outlier condition is met for all along-track errors up to $\sigma_{az,el} \approx 0.25°$. For the remaining parameters, as opposed to the previous example in the measurement space, the differences are now increasing for an increasing sensor noise, but there is no clear boundary at a certain sensor noise value. The larger the AT uncertainty, the larger also the acceptable sensor noise.

2.2.3 Observations – Time Bias Removal

As another approach to improve the association, it is attempted to use the advantages of the sensor coordinates of the measurements while mitigating the effect of the along-track error. This is done by first calculating the position differences between the catalogue and measured (ρ, az, el)-position in the curvilinear RTN for all detections in the tracklet. Because it is assumed that the along-track error is dominating and consistent between multiple detections, it is attempted to quantify the along-track error by averaging over the individual along-track errors which are affected by both the orbit and sensor noise. This mean along-track error $\overline{\Delta \mathrm{AT}}$ is then

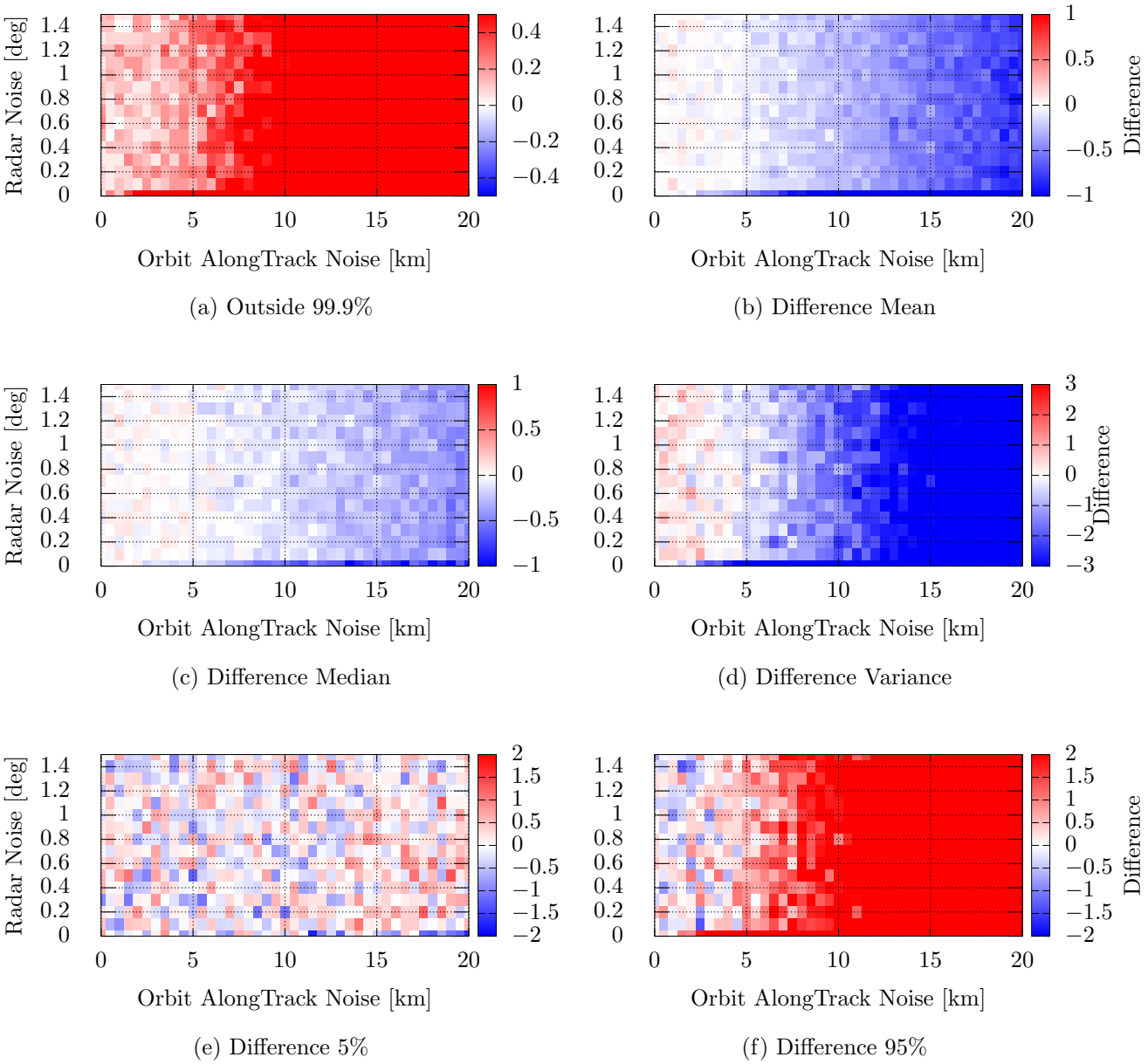

(a) Outside 99.9%

(b) Difference Mean

(c) Difference Median

(d) Difference Variance

(e) Difference 5%

(f) Difference 95%

Figure 2: Difference to the theoretically expected values of the M_{d}^2-distribution using the observables directly.

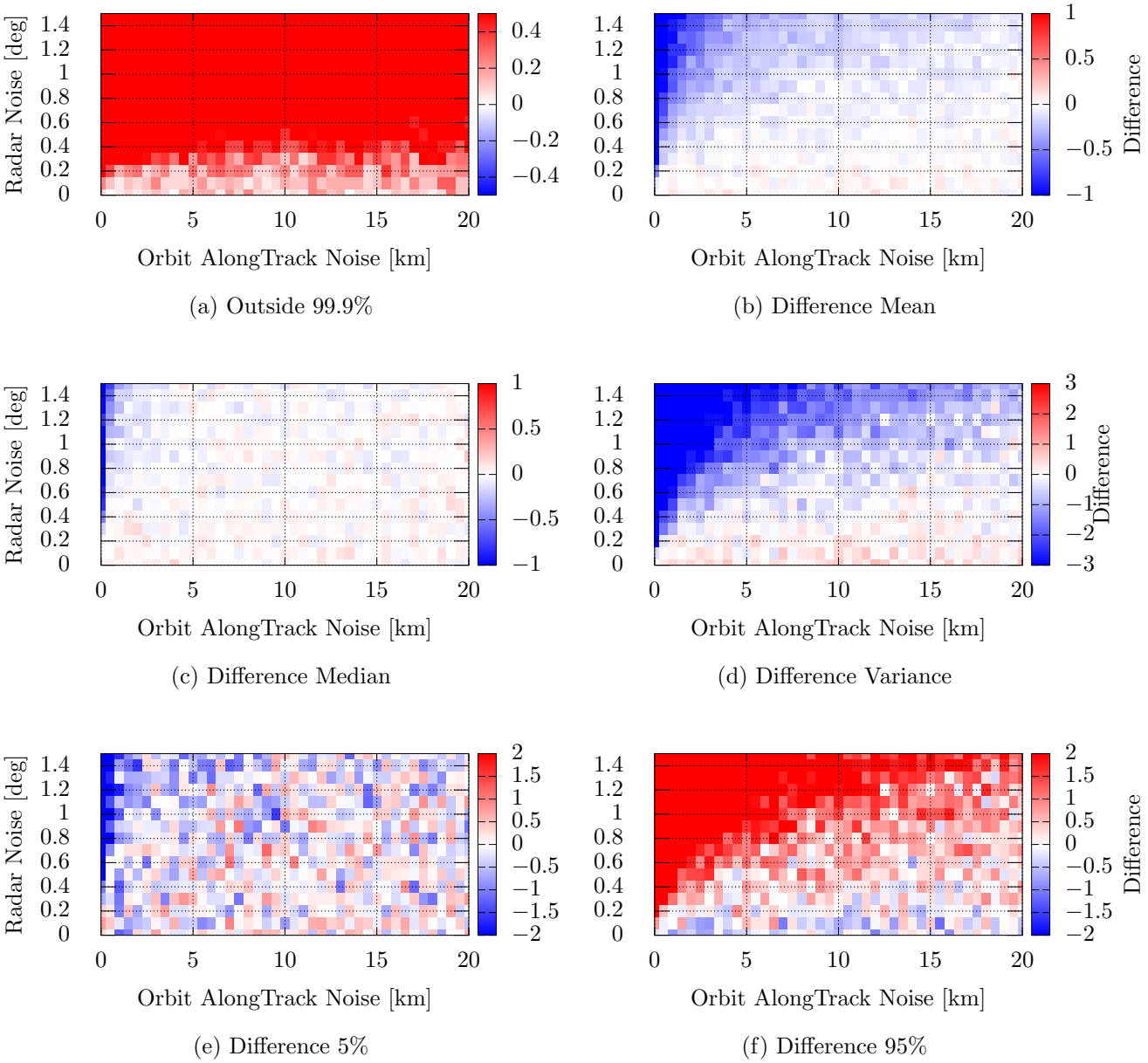

(a) Outside 99.9%

(b) Difference Mean

(c) Difference Median

(d) Difference Variance

(e) Difference 5%

(f) Difference 95%

Figure 3: Difference to the theoretically expected values of the M_{d}^2-distribution using the curvilinear RTN coordinates.

transformed to a time bias Δt_{AT} by dividing $\overline{\Delta \mathrm{AT}}$ by the total orbital velocity. The reference orbit from the catalogue is propagated by Δt_{AT} to correct the catalogue state before deriving the reference measurement from it for the comparison to the actual measurements. The uncertainty of the mean time bias Δt_{AT} is used as the new along-track orbit uncertainty and replaces the initial uncertainty of this component in the covariance matrix before transforming it to the measurement coordinates.

The results using this approach are shown in Figure 4. Concerning the general trend, it is visible that now the boundary towards a declining quality of associations is towards larger measurement noise and not towards larger along-track noise as in Figure 2 in the same coordinates. When comparing to the curvilinear coordinates in Figure 3, the results are in general worse now with the exception of the cases with large angular sensor noise and low along-track noise (top left corner). However, for this area the direct usage of the observations is better than the ones without the time bias and thus the removal of the time bias apparently does not improve the association.

2.2.4 Least Squares-based Time Bias Removal

Concerning the removal of the time bias, it is also attempted to use the high-precision range information as a useful information. For this, a least-squares problem is set up to minimise the range residuals by varying the time bias Δt_{AT} when propagating the reference orbit. The new along-track uncertainty is again derived via the fit, but it is very small now, thus the measurement errors dominate. The association is done in the measurements' frame as before. The results for tracklets with a length of 42 s and detections every three seconds (15 data points in total) are shown in Figure 5 and they are much better than the previous results even for large along-track errors. Because this fit is strongly dependent on the length of the tracklet and its density, the quality of the results might differ for different measurement scenarios. For the final association decision, also the size of the time bias compared to the expected along-track error would need to be considered in order to ensure that the correction value is not larger than expected, which is not done in this simplified test.

2.2.5 Summary

The conclusion from this analysis is that there is no single coordinate system which gives the best results, but depending on the conditions either the observable coordinates or the curvilinear RTN is better. Thus, it should rather be considered if there is either a relatively low noise sensor or a relatively high-confidence orbit. In general, the smaller covariance is the one which should be transformed to another system, because it has the better chance of remaining sufficiently normal. Another option would be to try to reduce the effect of a non-normal distribution by using Gaussian Mixture Models (GMMs) to approximate the non-normal distribution. For GMMs, a probability distribution is modelled by a sum of weighted normal distributions, which can be used to model any other distribution assuming a sufficient number of components is used. However, defining an equivalent of the Mahalanobis distance for GMMs which allows statistical gating does not seem to be available. Alternative distance measures such as the Kullback–Leibler divergence do not have the same statistical gating behaviour as the Mahalanobis distance and thus would need some additional calibration.

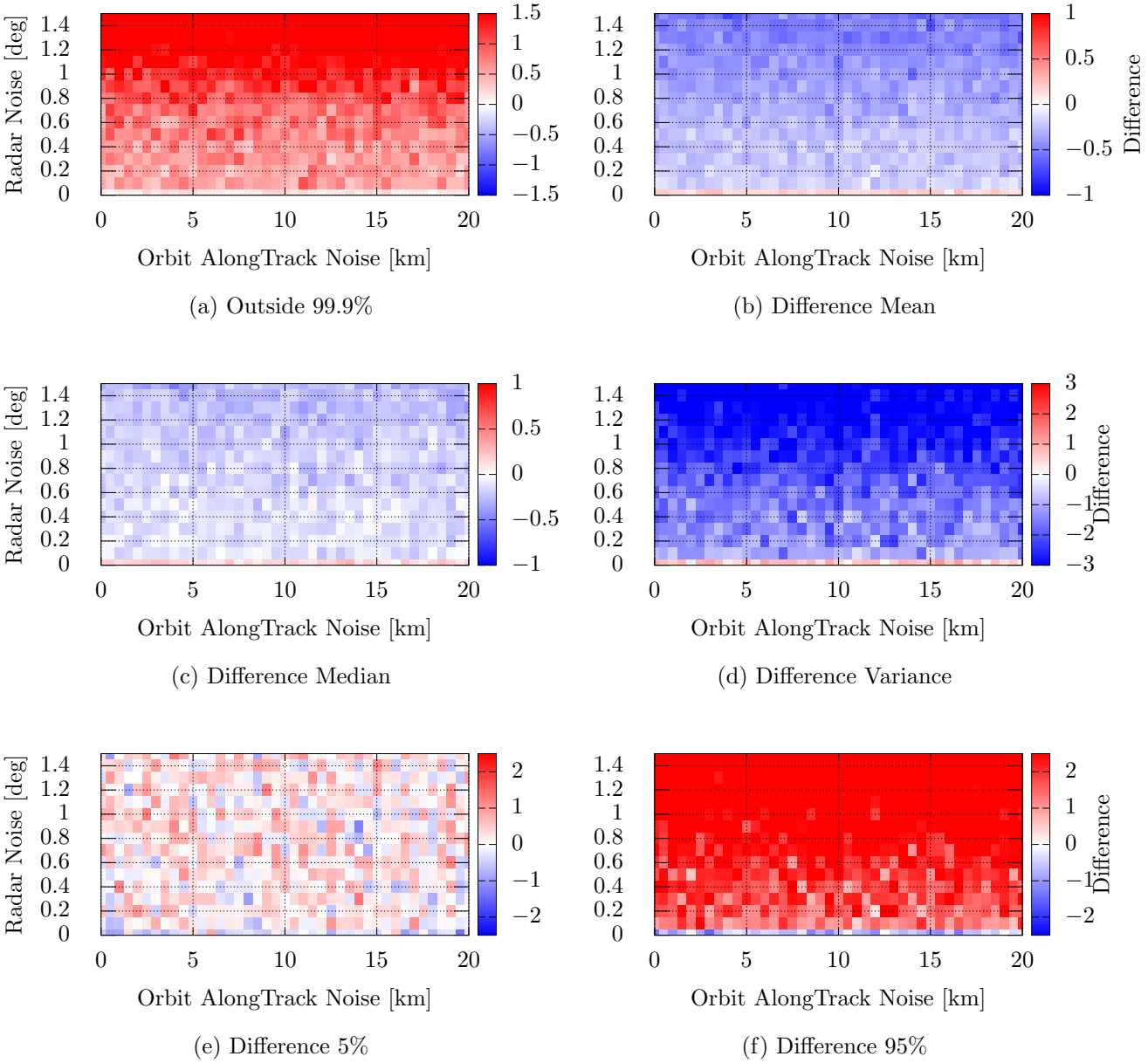

(a) Outside 99.9%

(b) Difference Mean

(c) Difference Median

(d) Difference Variance

(e) Difference 5%

(f) Difference 95%

Figure 4: Difference to the theoretically expected values of the M_{d}^2-distribution using the observables with the removed time bias.

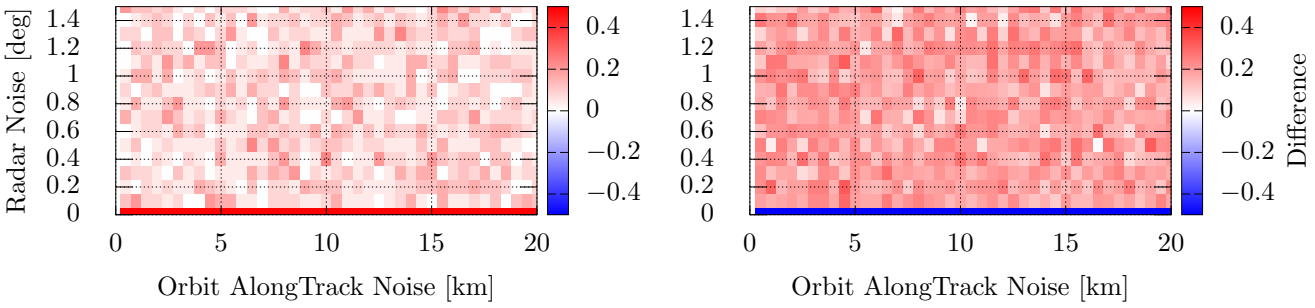

(a) Outside 99.9%

(b) Difference Mean

(c) Difference Median

(d) Difference Variance

(e) Difference 5%

(f) Difference 95%

Figure 5: Difference to the theoretically expected values of the M_{d}^2-distribution using the observables with the removed time bias via the least squares of the range residuals (tracklet length 42s, detection intervals 3s).

3 Object Confirmation and Maintenance

3.1 Overview

Within the catalogue build-up process, a decision has to be made whether and when a new object is introduced into the catalogue. This includes switching from tracklet-tracklet association to the previously discussed orbit-tracklet association for future observations of this object. This decision can be based on different parameters, which is discussed in the following.

The first approach for this is to use known track confirmation algorithms from multi-target tracking. A relatively simple one is to define N expected passes based on the current trajectory and then accept an object if m detections are made, thus m-out-N method [12]. Another option is the use of the sequential likelihood ratio test [13], which has already been applied to orbit cataloguing [14].

The second approach is the use of information theoretic measures. Such work is often based on [15]. Most applications in space surveillance have been performed with regard to sensor tasking, first by [16] and later extended by [17, 18]. Although sensor tasking might be considered to be related to cataloguing, this aspect rather covers the catalogue maintenance than the build-up.

In the following, information theoretic measures are used to make decisions on the confirmation of objects and their current quality. To distinguish further from the scheduling aspect, the work here focuses on survey sensors without dedicated tracking, e.g. a radar which is constantly scanning a pre-defined field of regard. This is also related to the previously introduced tracklet-orbit correlation, because it might include a first step of associating new tracklets with preliminary orbits before a decision concerning the status can be taken.

3.2 Object Confirmation - Theory

When a new object is created through the tracklet-tracklet correlation, an objective value based on the current information should be used to establish whether the orbital information for this object is good enough to include the object in the catalogue for regular maintenance. This means that its orbit needs to be sufficiently precise to perform the tracklet-orbit association reliably for a defined time span.

In practice, the quality of the orbit is dependent on several factors such as the number of passes, their geometry and their lengths. Due to the large variability and inter-dependence of these different parameters, it is preferred to have a characteristic value to quantify the available information and make it comparable between different cases with different conditions.

The most promising quantity from information theory is the differential entropy H of the probability density function $p(\vec{x})$ (in unit *bits*) [19]:

$$H(p(\vec{x})) = -\int_{-\infty}^{\infty} p(\vec{x}) \log_2 \left(p(\vec{x})\right) d\vec{x} \ . \qquad (2)$$

The smaller the entropy, the more information is available. For an n-dimensional multivariate normal distribution $\mathcal{N}(\vec{x}|\vec{\mu}, \Sigma)$ with mean $\vec{\mu}$ and covariance Σ, this can be solved analytically to:

$$H(\mathcal{N}(\vec{x}|\vec{\mu}, \Sigma)) = \frac{1}{2} \log_2 \left((2\pi e)^n \det\left(\Sigma\right)\right) \ . \qquad (3)$$

3.3 Object Confirmation - Experiments

As an initial experiment, it is attempted to relate the entropy of the state at the epoch of the least squares orbit determination (LSQ-OD) to the along-track uncertainty of the propagated covariance matrix after up to three days. The entropy of the state is calculated in Keplerian elements using the mean anomaly and also the propagation of the covariance is performed in that system because the error distribution keeps its Gaussian nature for a longer period of time in an orbital-elements-based system [7]. At each point of interest, this covariance can then be transformed to the curvilinear coordinates to get an along-track uncertainty.

To search for a relation between the differential entropy and the propagated size of the covariance, different conditions have been used for the tracklet length, the number of passes and the noise level of the observations based on the same group of LEO objects as in the previous chapter. Figure 6 shows the size of the covariance in along-track direction after 48 hours of propagation over the entropy at the orbit determination epoch. There are two different types of passes: those with a fixed number of observations (40s-5f: 40 s length with an observation every 5 s; 42s-3f: 42 s length with an observation every 3 s) and those with a random number of detections per pass (RanLen: 3-7 seconds between observations with 3-13 observations in total). For the random length, there is also an experiment with an increased angular noise of the sensor, $\sigma_{az,el} = 0.4°$ instead of $\sigma_{az,el} = 0.25°$. Additionally, there are LSQ-ODs from two and three passes. It is visible that the data clearly follows an overall trend where also the different measurement conditions overlap. This also shows that depending on the observation

geometry, an orbit which is calculated from three passes is not necessarily better than one using only two passes with a better observation geometry or temporal distribution. The use of the differential entropy seems to give a general measure of the available information and thus becomes independent of the specific parameters of an orbit determination.

As a second visualisation, Figure 7 shows the percentage of along-track uncertainties which are below 15 km as an example for the scenarios after 48 hours and 72 hours. Also here, it is visible that the different cases form a consistent trend, although there are some outliers. These plots show that it should be possible to give a statistical boundary of the propagated covariance based on the entropy of the covariance after the orbit determination.

The exact performance criterion for a database accepting σ_{T} as an along-track uncertainty after t days would depend on its application. If the goal is to maintain these objects' orbits by a given sensor network, these numbers would depend on the sensor characteristics, whereas a database for conjunction assessment would probably require other specifications. Thus, there is no intention of defining a threshold here, but only to show the usability of the entropy as a concept.

To test the combination of the object confirmation and orbit-tracklet association, an experiment was performed which included both the initial creation of the object and the association of subsequent observations. For each object, an LSQ-OD is performed with the first two passes and it is checked whether the differential entropy $H < -50$ bits, which is derived from the previous experiments. If $H > -50$ bits, the next pass is added to the LSQ-OD until the condition is met. It is assumed that the tracklet-tracklet correlation correctly identifies these candidates. After the orbit uncertainty is below the threshold, the resulting orbit is propagated to all later observations and the orbit-tracklet association is attempted in different coordinate systems. The total time span of simulated observations is seven days. The subsequent measurements are only used to test the association and they are not integrated into the orbit as an update. Only orbits and tracklets from the same objects are tested for an association, thus there is no possibility of a false positive result, meaning an association of a tracklet to an object which did not generate this tracklet.

The association is performed either in curvilinear RTN positions or measurement space. Four different approaches for the association are used in each coordinate system. The most simple one uses only one observation, independent of the total tracklet length, which serves mainly as a reference case. The other three are designed to use the entire information from the tracklet. The "Sum"-case uses the squared sum of the Mahalanobis distances over all m observations in the tracklet:

$$M^2_{d,total} = \sum_{i=1}^{m} M^2_{d,i} \ . \tag{4}$$

Theoretically in case of independent errors, this would lead to a $\chi^2(m \cdot \nu)$-distribution with the degrees of freedom equivalent to m times the degrees of freedom of the single observation (3 for curvilinear RTN and 4 for observations). Another approach is the "Time Bias Removal" (TBR) as explained in the previous section by minimising the range residuals via a least squares optimisation. As a third approach, the association is performed for each detection within the tracklet and the entire pass is accepted if more than a given percentage of observations in the tracklet have been positively correlated. This approach is called "Ratio" in the following. The association threshold for all tests is set at the cumulative value of 95% of the corresponding χ-distribution depending on the degrees of freedom.

Table 1: Success Rate of Orbit-Tracklet Association.

System		Random Length	40s-5f	42s-3f
Obs.	Single	92.2	86.2	87.1
	Sum	94.4	89.8	93.9
	TBR	85.2	76.1	76.0
	Ratio	96.7	92.9	94.4
Curvilinear RTN	Single	92.9	87.5	89.0
	Sum	97.1	93.3	96.8
	TBR	86.3	83.1	81.6
	Ratio	98.5	96.7	97.8

Tracklets with a fixed length (40s-5f and 42s-3f) and with random lengths as explained in the previous section are used for the simulation. The results are shown in Table 1. If the probability distributions were matched perfectly, it would be expected to have exactly 95% of positive associations for the cases Single, Sum and TBR. The case Ratio should have 100%. It can be seen in the table that the actual association rates are slightly lower which is probably due to wrong estimates of the covariance after OD and propagation. Especially, the time bias removal is not even reaching 90% for any of the experiments.

Some additional plots are used to analyse the reasons. Figure 8 shows the percentage of true positive (TP) and false negative (FN) associations over

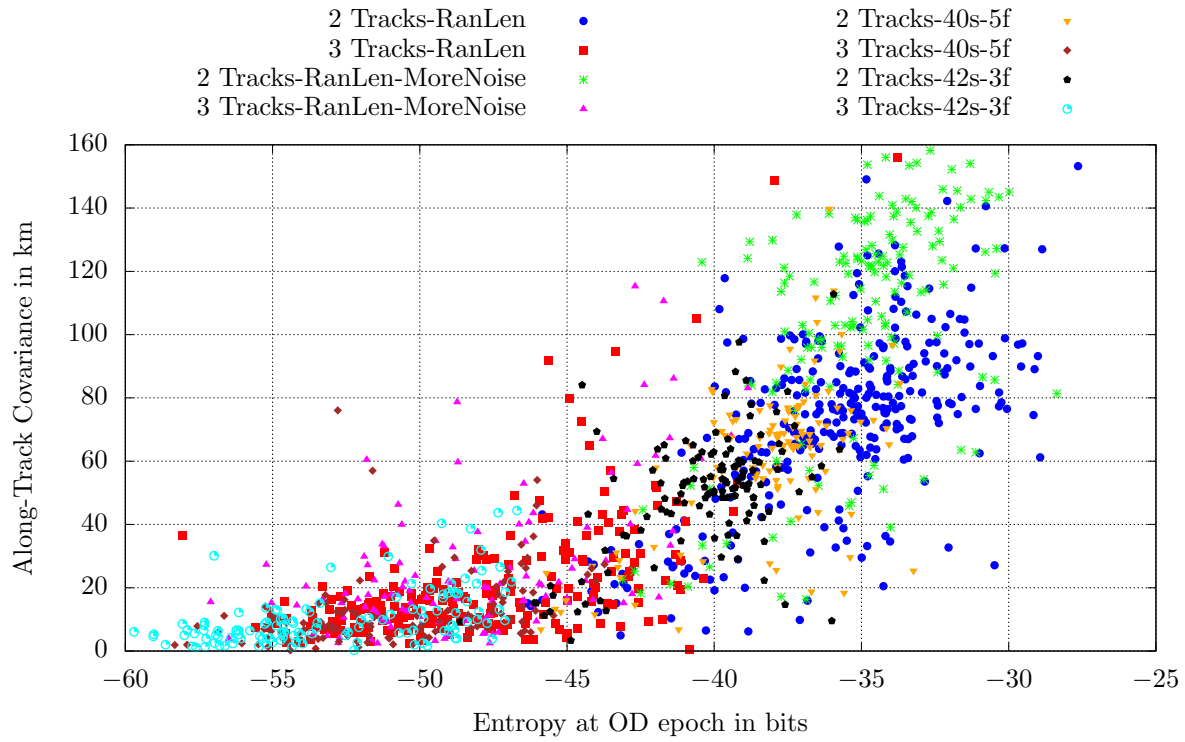

Figure 6: Entropy at OD epoch and the resulting along-track covariance after 48 hours for different cases.

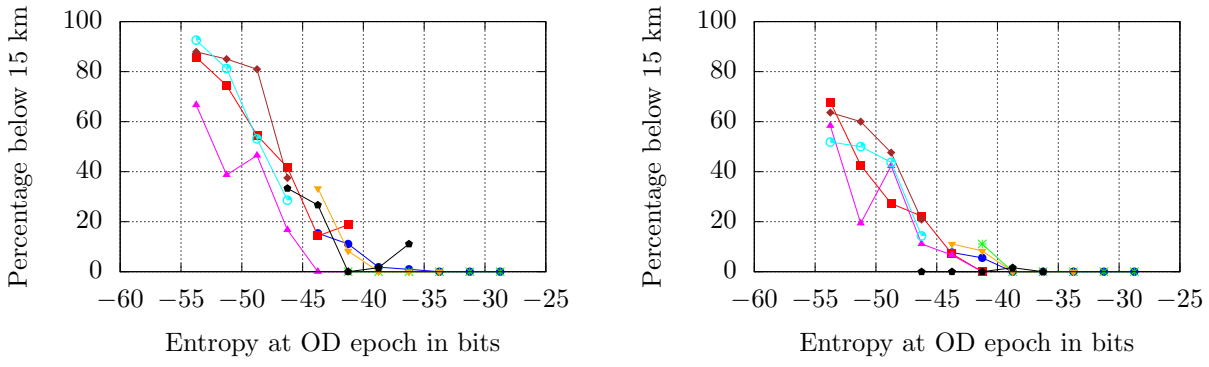

(a) 48 hours

(b) 72 hours

Figure 7: Entropy at OD epoch and the resulting percentage of along-track covariance below 15 km for different cases.

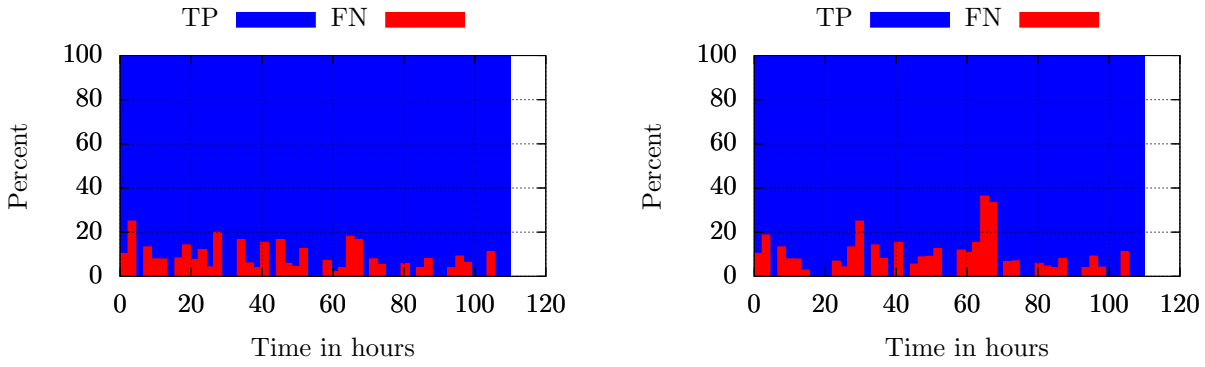

(a) Curvilinear RTN

(b) Observation

Figure 8: Percentage of TP and FN over the time between LSQ-OD and association.

the time between the LSQ-OD epoch, i.e. the orbit's reference epoch, and the epoch of the observation for the association of the single observations in both coordinate systems. True positives are successful associations, while false negative means that the association was falsely rejected. It can be seen that there is no trend of an increased FN percentage with more time between the orbit's reference epoch and the measurement. Figure 9 shows the same data set over the difference between the along-track error ΔAT calculated from the known true reference position of the object and the along-track component σ_{T} of the covariance matrix. From these plots, it can be seen that a FN association is more likely if ΔAT is larger than σ_{T}, which also makes sense intuitively.

Additionally, the distribution of the Mahalanobis distances of the associations can be plotted to compare it to the theoretically expected χ-distribution with the corresponding degrees of freedom. Figure 10 depicts this comparison for the association of the single observations. In both cases, it can be seen that the theoretical distribution is roughly matched. Thus it can be suspected that the majority of the failed associations is due to outliers and not due to a general shift of the statistical distribution.

Using the "Sum"-approach, it had been mentioned that the degrees of freedom are equivalent to the product between the degrees of freedom of the single observation and the number of observations in the tracklet under the assumption of uncorrelated errors. However in the orbit-tracklet-association both the errors within one detection and the errors of the different observations within one pass are not statistically independent. Thus it can be seen from Figure 11, that the distribution is shifted to lower values as it effectively has less degrees of freedom, which also explains why the Sum-approach had the largest percentage of TP-associations.

3.4 Object Quality - Theory

To extend the work on the orbit-tracklet association, the measurements should also be used to give an impression on the current quality of the catalogue object. This parameter should reflect both the current uncertainty of the orbit and the newly received measurements as a feedback by comparing them to the expected ones based on the current orbit.

From the framework of the information theory, a property of an uncertain event from a probability distribution is the *surprisal* (or *information content*). This is used to emphasise that events with a lower probability contain more information if they occur, because they might lead to changes in the current models or assumptions. The surprisal of an event x_k with a probability $\mathcal{P}(x_k)$ is defined as (in bits):

$$I(x) = -\log_2\left(\mathcal{P}(x_k)\right) \ . \tag{5}$$

The entropy H, which was used in the previous sections, is the expectation value of the surprisal:

$$\mathrm{E}\left[I(x)\right] = H(p(x)) \ . \tag{6}$$

From these definitions it can be seen that an event with $\mathcal{P}(x_k) = 0$ has infinite surprisal, whereas an event with $\mathcal{P}(x_k) = 1$ has no surprisal and thus also contains no information. Classically, this concept is used for discrete probability distributions.

To transfer this to the continuous probability density functions used in the present problem, a definition of p_z has to be found as the *pseudo-probability* of the new measurement z_m, which fulfils the conditions above, while considering the uncertainty of both, the measurement and the state. This

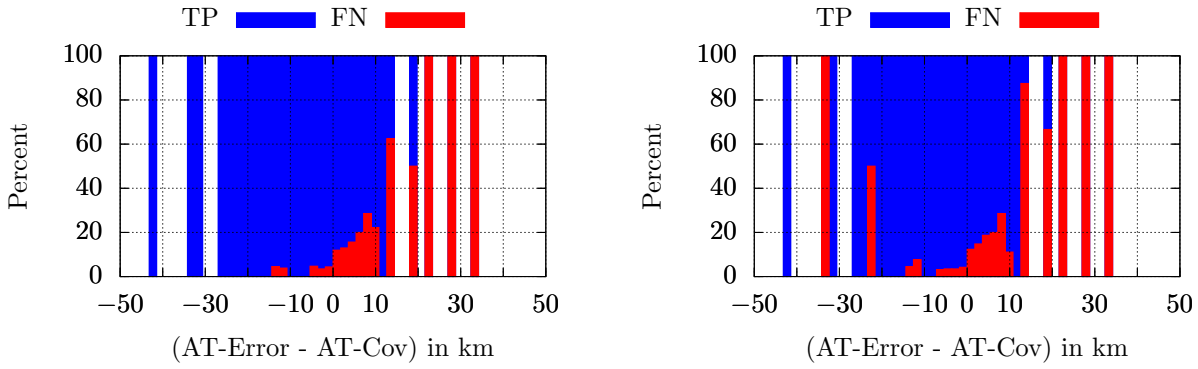

(a) Curvilinear RTN (b) Observation

Figure 9: Percentage of TP and FN over the difference between the along-track component of the covariance and the present along-track error.

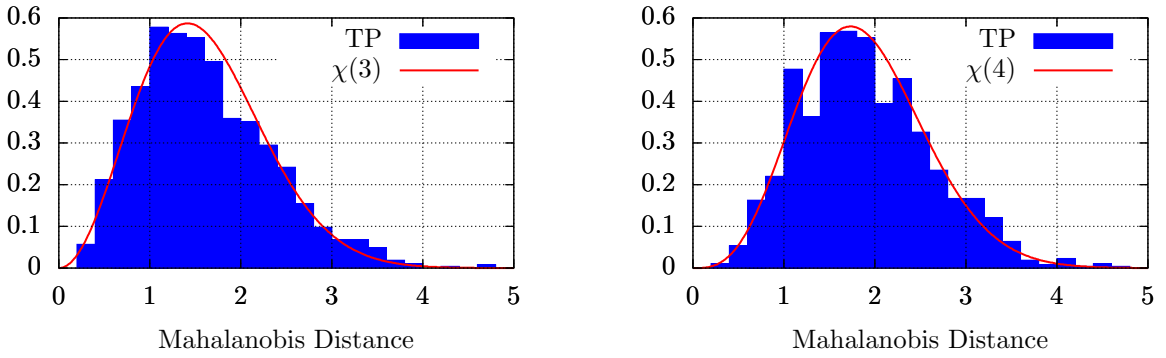

(a) Curvilinear RTN (b) Observation

Figure 10: Mahalanobis distance compared to reference χ-distribution for single observations (Random Len).

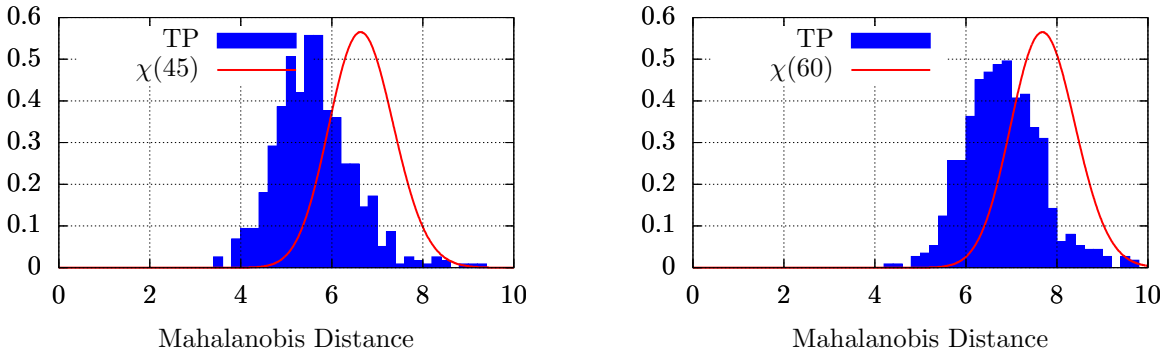

(a) Curvilinear RTN (b) Observation

Figure 11: Mahalanobis distance compared to reference χ-distribution for the "Sum"-approach of single observations (42s-3f).

leads to the following equation:

$$p_z = \int_{-\infty}^{\infty} \sqrt{\mathcal{N}(\vec{z}|\vec{z}_e, \Sigma_{x,M} + \Sigma_M) \cdot \mathcal{N}(\vec{z}|\vec{z}_m, \Sigma_M)}\, d\vec{z}\,, \tag{7}$$

where $\mathcal{N}(\vec{z}|\vec{z}_e, \Sigma_{x,M} + \Sigma_M)$ is the assumed normal distribution of the expected measurement $\vec{z}_e$ based on the current state. The uncertainty of this distribution is taken from the sum of the measurement uncertainty Σ_M and $\Sigma_{x,M}$, which is the state's uncertainty Σ_x projected into the measurement space. The distribution $\mathcal{N}(\vec{z}|\vec{z}_m, \Sigma_M)$ is the one around the newly received measurement $\vec{z}_m$ with the measurement uncertainty Σ_M. This definition fulfils the criterion to be equal to 1 only if the two distributions are exactly the same, meaning that there is no uncertainty on the state and the expected measurement is matched exactly. If there is no overlap between the distributions, this value is 0. Although, Equation 7 uses the normal distribution as an example, any probability distribution can be used. The value p_z is mathematically not a probability because its integral over all possible realisations of the measurement $\vec{z}_m$ is larger than one. However, it is also possible to use this integration over all $\vec{z}_m$ to find a normalisation constant which can be used to give p_z the properties of a probability distribution. Due to the log-operation of the surprisal, this normalisation would only lead to a constant offset, which will not be considered in the following. Thus, the surprisal is calculated as:

$$I(z) = -\log_2(p_z)\ . \tag{8}$$

This leads to measurements with a low surprisal if there is a small state uncertainty and the measurements are close to the expected ones. The integral for p_z can either be multidimensional and consider all observables or use only the most precise measurement as this provides the most information. In case of the radar, this is the range.

The idea behind this selection is that it considers both the difference between the expected and received measurement (Δz) and indirectly also the size of the state uncertainty. The larger the state uncertainty, the larger also the minimum achievable surprisal, which makes sense considering that an object with a large uncertainty should not be a high-quality object with a low surprisal. At the same time, the surprisal also becomes sensor-dependent if there are different noise levels between sensors. For most cases, a more precise sensor can produce measurements with a higher level of surprisal because it can sample the uncertainty area at a finer resolution. In principle it could be possible to compare different sensors' minimum surprisal values based on the same orbit and observation geometry.

The behaviour of the surprisal is visualised in Figure 12 for an example with an along-track error of a few kilometres which dominates the range uncertainty compared to the sensor's measurement uncertainty. The sensor's noise and the difference compared to the expected measurement Δz (called error in the plot) is varied systematically. It is visible that for a given measurement error Δz the surprisal reduces with an increased sensor noise, because the reliability and thus the information content of the measurement reduces. If the sensor noise is fixed, the surprisal is the least for $\Delta z = 0$, because this confirms the current estimate of the orbit and thus has the smallest possible information gain. As can be seen in the plot, the difference Δz is much larger than the sensor noise, thus the variance due to the sensor noise is only leading to minor variations of the surprisal.

One possibility to remove the sensor-dependency would be to normalise the surprisal by the minimum surprisal of the sensor, which is calculated as $I_{Sensor,0} = I(z_m = z_e)$.

To further analyse the variability of the surprisal, a Monte Carlo experiment was conducted for a single state with a covariance matrix in RTN coordinates. The measurements were generated after the actual state error was randomly sampled from the state covariance. For each range measurement, the surprisal is calculated. The results are given by the plot "Ref" in Figure 13, which shows the variation of the surprisal due to different realisations of the along-track error. As a comparison, the same calculation has been performed under the assumption that the current estimate of the covariance is only half of the sampled one, thus overly optimistic. This leads to two opposing effects. In cases where the actual along-track error is small enough to be consistent even with the smaller covariance, it leads to smaller values of the surprisal because the uncertainty is less. At the same time, the tail of the surprisal values in the histogram becomes more pronounced because the measurements with larger offsets are unexpected and thus contain more information. This second case, when the error is larger than what would be consistent with the covariance matrix, is the one which should be detected and as it can be seen the surprisal is a possible tool for that.

3.5 Object Quality - Experiment

To test the proposed parameter, the same experiment setup as in the previous chapter has been used. The orbit determination is performed on subsequent

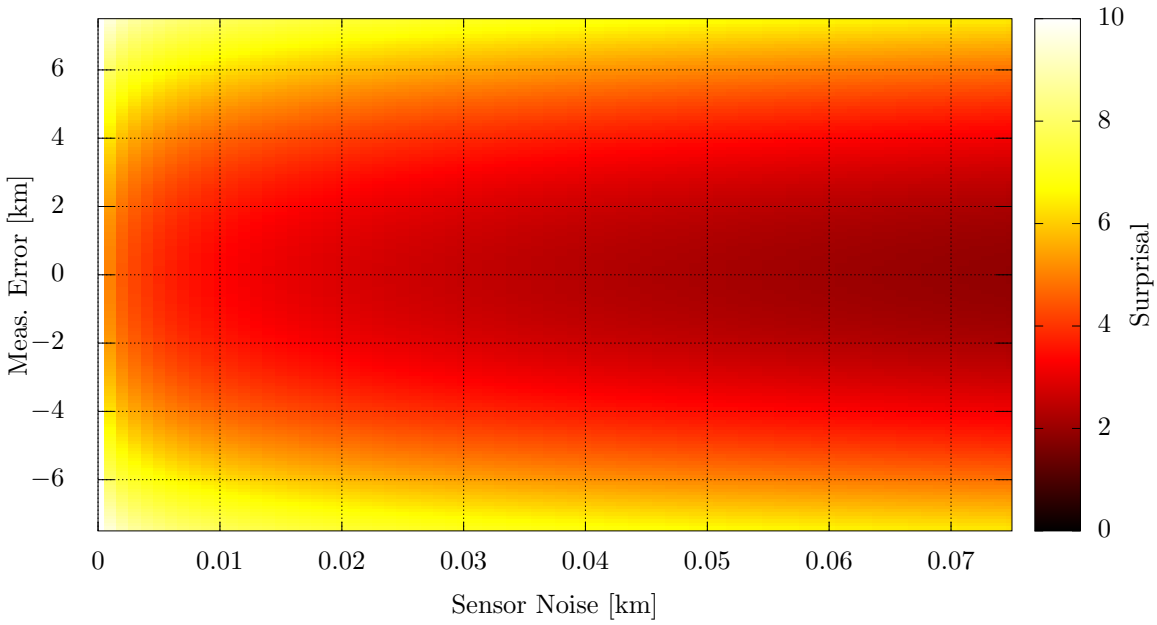

Figure 12: Surprisal over different sensor noise level and the offset (error) compared to the expected measurement.

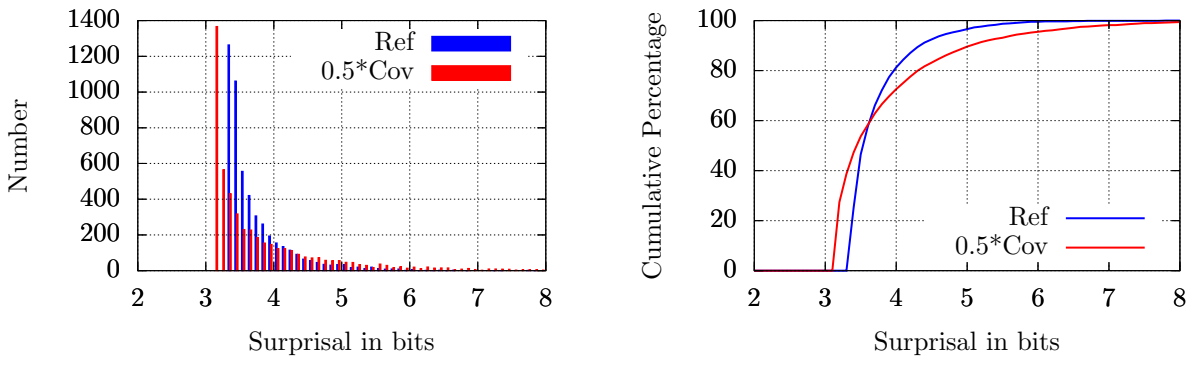

(a) Histogram

(b) Cumulative

Figure 13: Experiment comparing the reference results to those obtained with a covariance of half the actual size.

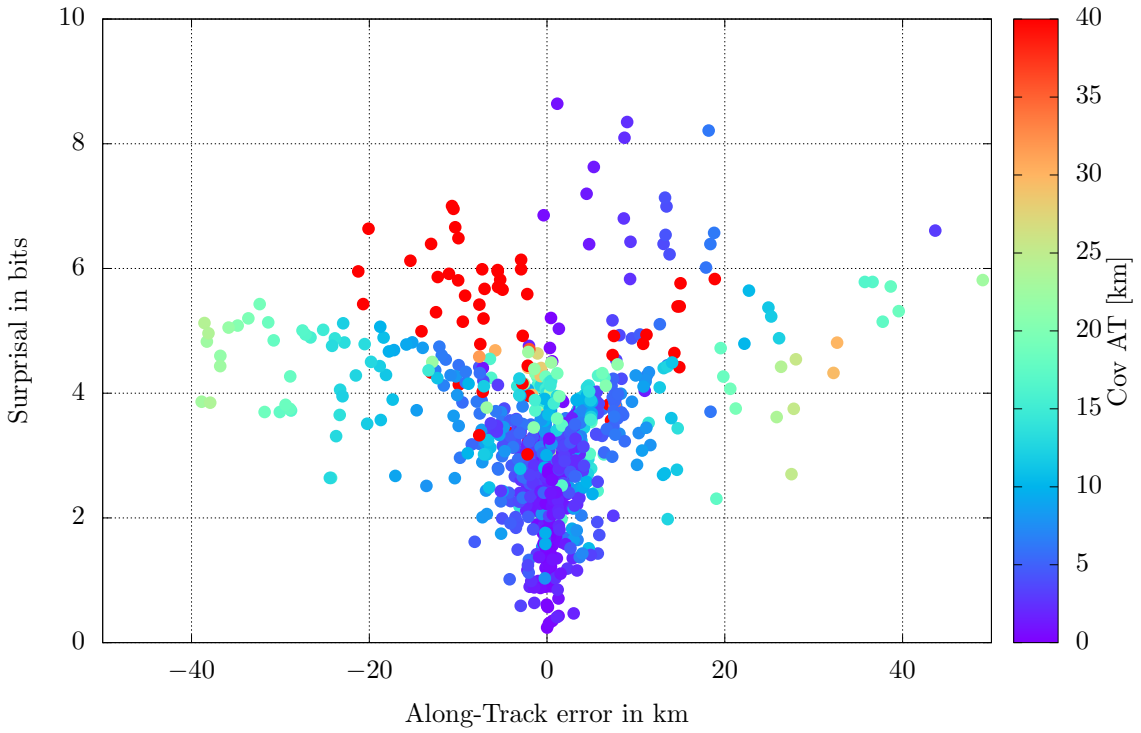

Figure 14: Surprisal over along-track error and covariance using propagated orbits from the orbit determination.

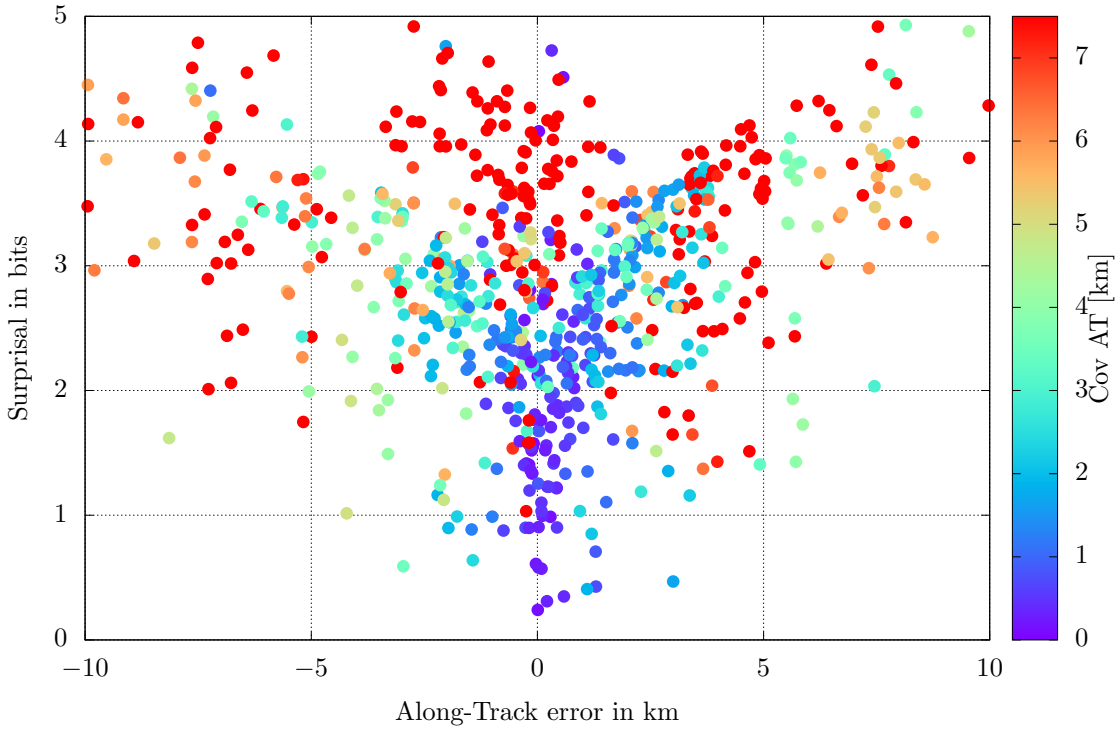

Figure 15: Surprisal over along-track error and covariance using propagated orbits from the orbit determination (zoom).

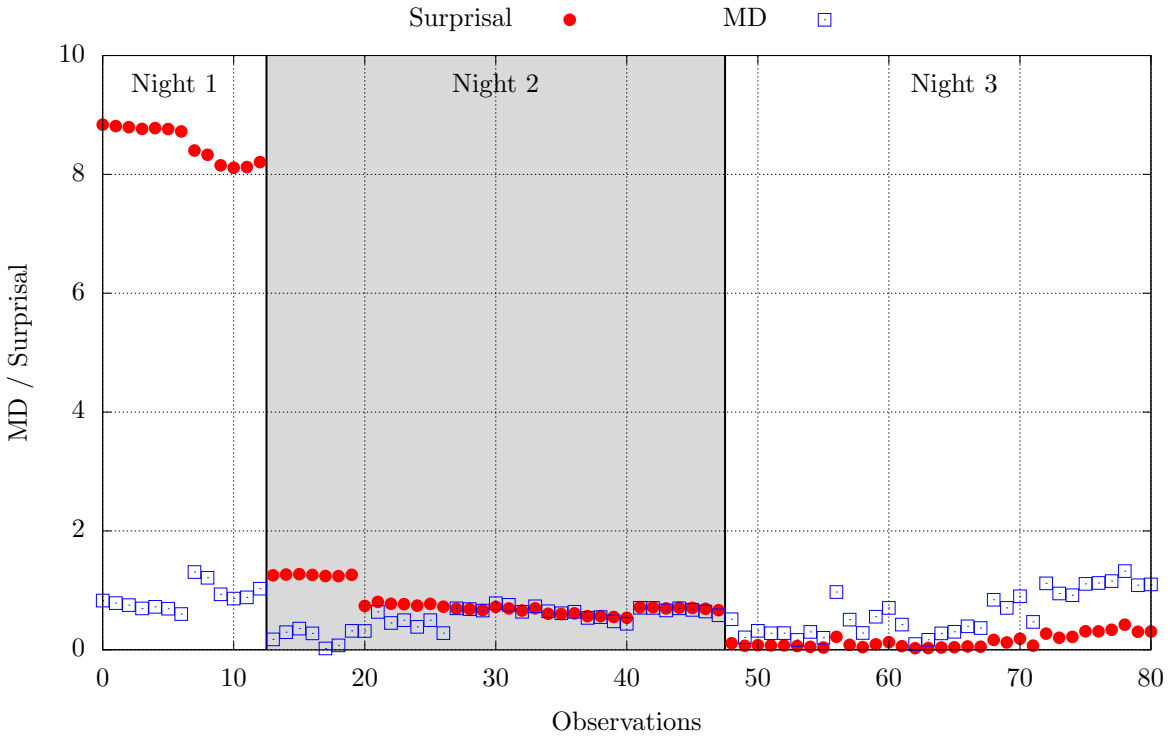

Figure 16: Development of Mahalanobis distance and surprisal over three nights.

tracklets until $H < -50$ bits and the resulting orbit is then propagated to all following measurements. Here, also the surprisal is calculated as described for each new measurement.

The results are shown in Figure 14 with the along-track error calculated from the (in the real case unknown) true position on the x-axis and the size of the along-track covariance as a colour code. The surprisal is again calculated by using only the range measurement. It can be seen that very low values of the surprisal are reached for small along-track errors and covariances as expected. The zoomed version in Figure 15 also shows that objects with a low along-track error but a large covariance lead to a larger surprisal, because they contain more information.

Another example using real optical measurements is shown in Figure 16. In this case of a GEO satellite, an orbit has been determined from one night of measurements using the LSQ-OD. For the next three nights, this orbit is propagated to the new measurement epochs and the Mahalanobis distance for the association can be calculated together with the surprisal. The association and the surprisal both use the two-dimensional observation vector of right ascension and declination. After each night, the orbit is updated using the newly associated measurements. The Mahalanobis distance in the plot is relatively stable between one and two, because the differences between the expected and received measurement are scaled by the covariance. If both are decreasing, the Mahalanobis distance remains at similar values. In contrast to that, the surprisal considers the size of the covariance, which is shrinking after each night due to the incorporation of new measurements. For the second and third night there are clear decreases in the surprisal compared to the previous night, which indicates that the confidence in the object and its position has in fact increased.

4 Conclusion

In this work, an analysis of three aspects of the automated maintenance of a space object orbit database has been presented. The first part considered the association of new measurements with existing catalogue objects. It was shown how the effects from the orbit and sensor noise restrict the choice of an appropriate coordinate frame for the comparison. It was also tested how an entire tracklet might be treated compared to a single point. In the second part, the use of measures from information theory to build and maintain the database have been introduced. The parameters entropy and surprisal can generalise the information content for spe-

cific objects and measurements. This can be used to either assess whether an initial orbit is good enough to be integrated into the database or to check the quality of an object's orbit.

Future work can include further tests with regard to the confirmation of new objects, which may consider more than just the covariance. The feedback from associated measurements to estimate the current quality can be extended to have a direct impact on the tracking time during the current pass or the future scheduling.

Acknowledgements

The first author is supported by the European Space Agency through the Networking/Partnering Initiative.

References

[1] J.-C. Liou, N. L. Johnson, Risks in Space from Orbiting Debris, Science, 311 (2006) 340–341.

[2] B. Reihs, A. Vananti, T. Schildknecht, A Method for Perturbed Initial Orbit Determination and Correlation of Radar Measurements, Advances in Space Research, 66 (2020) 426 –443.

[3] P. Mahalanobis, On the generalised distance in statistics, Proceedings of the National Institute of Science of India, 2 (1936) 49–55.

[4] C. Früh, T. Schildknecht, R. Musci, M. Ploner, Catalogue correlation of space debris objects, Proceedings of the 5th European Conference on Space Debris, Presented paper, Darmstadt, Germany, April 2009.

[5] J. A. Siminski, T Flohrer, Comparison-space selection to achieve efficient tracklet-to-object association, Advances in Space Research, 64 (2019) 1423–1431.

[6] D. A. Vallado, S. Alfano, Curvilinear coordinate transformations for relative motion, Celestial Mechanics and Dynamical Astronomy, 118 (2014) 253–271.

[7] K. Hill, C. Sabol, K. T. Alfriend, Comparison of covariance based track association approaches using simulated radar data, The Journal of the Astronautical Sciences, 59 (2012) 281–300.

[8] A. Vananti, T. Schildknecht, Distance between Keplerian orbits in the correlation of short arc radar tracks, KePASSA Workshop, Logroño, Spain, April 2019.

[9] D. Giza, P. Singla, J. Crassidis, R. Linares, P. Cefola, K. Hill, Entropy-based space object data association using an adaptive Gaussian sum filter, AIAA/AAS Astrodynamics Specialist Conference, 2010.

[10] I. I. Hussein, C. W. Roscoe, M. P. Wilkins, P. W. Schumacher, On mutual information for observation-to-observation association, 2015 18th International Conference on Information Fusion, IEEE, 2015, pp. 1293–1298.

[11] M. Abramowitz, I. A. Stegun, Handbook of mathematical functions: with formulas, graphs, and mathematical tables, *Vol. 55*, Courier Corporation, 1965.

[12] Y. Bar-Shalom, K.-C. Chang, H. M. Shertukde, Performance evaluation of a cascaded logic for track formation in clutter, Conference Proceedings., IEEE International Conference on Systems, Man and Cybernetics, IEEE, Cambridge (MA), USA, November 1989, pp. 13–17.

[13] S. Blackman, R. Popoli, Design and analysis of modern tracking systems, Artech House, Norwood (MA), USA, 1999.

[14] M. Pittelkau, False-Object Identification for Space Surveillance Catalog Maintenance, Advanced Maui Optical and Space Surveillance Technologies (AMOS) Conference, Presented Paper, Maui (HI), USA, September 2016.

[15] A. Rényi et al., On measures of entropy and information, Proceedings of the Fourth Berkeley Symposium on Mathematical Statistics and Probability, Volume 1: Contributions to the Theory of Statistics, The Regents of the University of California, 1961.

[16] C. M. Kreucher, K. D. Kastella, A. O. Hero III, Information-based sensor management for multitarget tracking, Signal and Data Processing of Small Targets, *Vol. 5204*, International Society for Optics and Photonics, 2004, pp. 480–489.

[17] K. J. DeMars, M. K. Jah, Evaluation of the information content of observations with application to sensor management for orbit determination, AAS/AIAA Astrodynamics Specialist Conference, Girdwood (AK), USA, August 2011.

[18] M. J. Gualdoni, K. J. DeMars, An Improved Representation of Measurement Information Content via the Distribution of the Kullback-Leibler Divergence, AAS/AIAA Astrodynam-

ics Specialist Conference, Univelt Inc., Stevenson (WA), USA, August 2017.

[19] T. M. Cover, Elements of information theory, Wiley-Interscience, Hoboken, N.J, 2006.